

THE EFFECT OF THE STARTING MATERIAL ON THE THERMAL DECOMPOSITION OF IRON OXYHYDROXIDES

*A. C. Oliveira*¹, *G. S. Marchetti*² and *M. do Carmo Rangel*^{1*}

¹GECCAT, Instituto de Química, Universidade Federal da Bahia, Campus Universitário de Ondina, 40170-290 Salvador, Ba, Brazil

²CINDECA, Facultad de Ciencias Exactas, Universidad Nacional de La Plata, 1900, 47 y 115, La Plata, Argentina

(Received August 2, 2002; in revised form February 7, 2003)

Abstract

The effect of the iron precursor on the thermal decomposition of iron oxyhydroxides was studied by DSC, DTA and TG in this work. Samples were prepared from iron nitrate, iron sulfate and iron chloride and the thermal curves obtained were analyzed by specific area measurements, X-ray diffraction and Mössbauer spectroscopy. It was found that the iron oxyhydroxide precursors affect the temperatures of the hematite formation as well as the textural properties of the final hematite producing particles with different diameters as following: iron sulfate (3.3 nm) << iron nitrate (15 nm) < iron chloride (24 nm).

Keywords: Fe(III)hydrite, hematite, iron chloride, iron nitrate, iron oxide, iron sulfate

Introduction

Iron oxides are an important group of catalysts due to their chemical properties and low cost. They have been extensively studied for several applications [1–3]. In the catalysis field, they have been used in many industrial processes as ammonia synthesis [4], water-gas shift reaction [5, 6] and Fischer–Tropsch synthesis [7] among others.

In all cases, the thermal methods can provide useful information about the characteristics and properties of the catalysts which in turn determine their applications as well as the best conditions of their operation. One of the most important study concerning the thermal analysis of catalysts is related to the monitoring of the catalyst production from its precursor. The profile of the thermal curves can often be used to get information about the textural and other characteristics of the catalysts which in turn can be related to catalytic properties. However, the iron precursor can affect the thermal curves and thus make this analysis more difficult.

In order to overcome this problem, the effect of the iron precursor on the thermal curves was studied in this paper. Samples were prepared from iron nitrate, iron sul-

* Author for correspondence: E-mail: mcarmov@ufba.br

fate and iron chloride and the thermal curves were analyzed with the aim of chemical analysis, specific area measurements, X-ray diffraction and Mössbauer spectroscopy.

Experimental

Samples were prepared by precipitation techniques at room temperature using iron nitrate (N sample), iron sulfate (S sample) and iron chloride (C sample). Aqueous solutions of the iron precursor (1N) and of ammonium hydroxide (25% w/w) were added to a beaker with water, under stirring. The final pH was adjusted to 11 and the system was kept under stirring for 30 min. The sol produced was centrifuged (2000 rpm, 5 min), rinsed with water to remove the anions from the starting material and dried at 120°C.

The DSC experiments were carried out in a DSC/DTA/TG 50 model Shimadzu equipment, under nitrogen flow (100 mL min⁻¹) at a heating rate of 10° min⁻¹ from room temperature up to 600°C, using around 2 mg of the sample in a closed crucible. TG and DTA experiments were performed in the same equipment and in the same conditions but heating the samples up to 1000°C.

In order to identify the peaks of the DSC curves some values of temperatures were selected, as shown in Fig. 1. The solids were heated, in independent experiments, at 10° min⁻¹ and kept at the desired temperature for 2 h, under nitrogen flow (100 mL min⁻¹). The samples were characterized by chemical analysis (N, S, Cl), specific area measurements, X-ray diffraction and Mössbauer spectroscopy.

The sulfur and nitrogen contents in the solids were determined using a model FlashEa 1119 Thermofinnigan equipment. Samples (15 mg) were dried at 90°C for 2 h, mixed with vanadium pentoxide (15 mg) and then analyzed. Before the analysis, a calibration curve was obtained using 2 mg of sample in a tin capsule. The chloride amount was measured by the Volhard method [8]. A silver nitrate solution was added to the sample previously dissolved in concentrated nitric acid until a white precipitate is produced. The solution was titrated with a sodium thiocyanate solution.

X-ray diffractograms were got at room temperature with a model XD3A Shimadzu instrument using CuK_α radiation generated at 40 kV and 20 mA. The specific area (BET method) were measured in a model TPD/TPO 2900 Micromeritics equipment from samples previously heated under nitrogen (150°C, 1 h).

The Mössbauer spectra were obtained in transmission geometry, with a 512-channel constant acceleration spectrometer at room temperature. A source of ⁵⁷Co in Rh matrix of nominally 50 mCi was used. Velocity calibration was performed vs. a 12 μm thick α-Fe foil. All isomer shifts mentioned in this paper are referred to this standard at 298 K. The temperature between 22 and 298 K was varied using a Displex DE-202 Closed Cycle Cryogenic System. The spectra were evaluated by using a least-squares nonlinear computer fitting program with constraints. Lorentzian lines were considered with equal widths for each spectrum component. The spectra were folded to minimize the geometric effects. All spectra were fitted with a program including hyperfine-parameters distributions to account for the different particle sizes and/or crystallographic sites of the iron phases.

Results and discussion

Figure 1 shows the DSC curves with the selected temperatures, the specific areas and the results of chemical analysis of the solids heated at each temperature. It can be seen that the specific area of the sample prepared from iron nitrate (N sample) decreased with the increasing temperature until 310°C; however it increased with a higher temperature achieving a value of 142 m² g⁻¹ which is close to the area of the solid heated at 150°C. The X-ray diffractogram of this sample heated at 150°C displayed two amorphous halos as shown in Fig. 2. The Mössbauer spectra of N150 consist of a quadrupole-split doublet, at 298 K, and a sextet at 22 K. Both signals have broad lines. Their parameters (Tables 1a and 1b) can be assigned to a 'poorly-crystallized' Fe(III)hydrite and/or lepidocrite (γ -FeOOH) [9, 10]. Considering: (i) the presence of hematite (α -Fe₂O₃) at a temperature higher than 150°C and (ii) the struc-

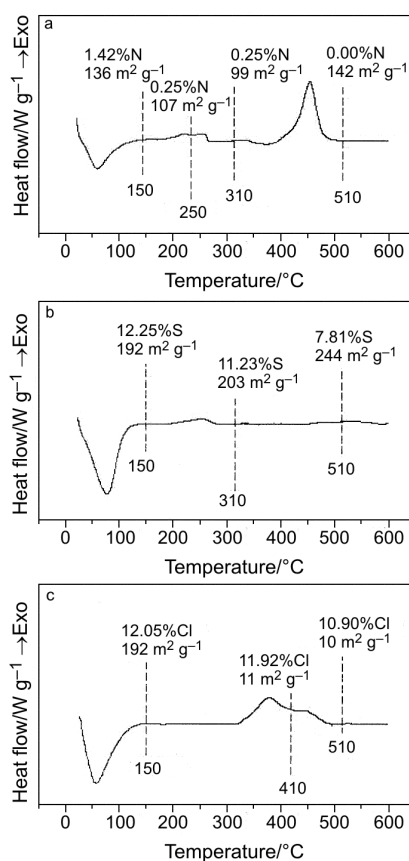


Fig. 1 DSC curves of iron oxyhydroxide prepared with a – iron nitrate (N sample), b – iron sulfate (S sample) and c – iron chloride (C sample). The specific area of the solids and the amounts of nitrogen (N), sulfur (S) and chloride (Cl) at selected temperatures are also shown

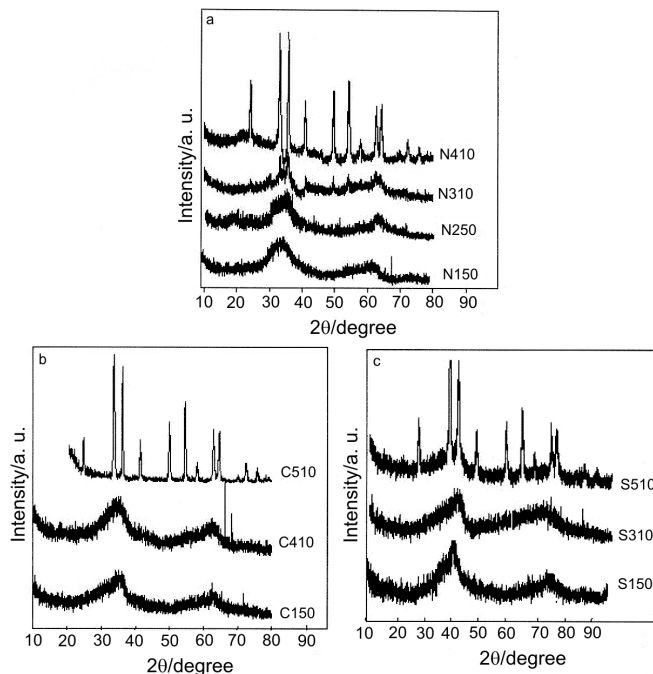


Fig. 2 X-ray diffractograms of iron oxyhydroxide prepared with a – iron nitrate (N sample), b – iron sulfate (S sample) and c – iron chloride (C sample) after heating at selected temperatures

ture of Fe(III)hydrite is related to that of hematite, with hexagonal close packing of oxygen and Fe^{3+} occupying the octahedral interstices, we can conclude that N150 sample is Fe(III)hydrite. By comparing these results with the TG profile (Fig. 3a) and with the Mössbauer spectra of the sample before heating, we can see that there is a strong loss of mass (41.204%) but no phase change. Therefore, the first endothermic peak can be assigned to the loss of volatile compounds in accordance with other works [11, 12]. Similar X-ray pattern, Mössbauer spectra and loss of mass were found for N250. The increase of the hyperfine magnetic field (Table 1b) and the decrease of the width lines in the Mössbauer spectrum at 22 K indicate an increase of the crystallinity of the sample. Besides, a decrease of specific area was noted, showing that the coalescence of particles and/or porous occurred simultaneously with the loss of volatile. At 310°C, the solid produced an X-ray diffractogram with some peaks typical of hematite. The Mössbauer spectrum of the N310 sample at 298 K shows a central quadrupole doublet and a magnetic sextet. The parameters of the sextet correspond to hematite (Table 1a). This signal represents 12% of the spectrum. At 22 K it is not possible to distinguish the presence of $\alpha\text{-Fe}_2\text{O}_3$ due to the broad Fe(III)hydrite sextet. Therefore, we can deduce that the shoulder detected by DSC, in the range of 200–300°C (Fig. 1a), is related to the beginning of the hematite formation. At 510°C, the solid showed the X-ray pattern of hematite and it was confirmed

by the Mössbauer spectrum at 298 K, as it is shown in Table 1. It means that the peak centered at 450°C, in DSC pattern, can be assigned to the crystallization of hematite. As we can see from the TG curve, this process is not followed by the loss of mass. By comparing the DSC curve with the DTA one (Fig. 3b), we can see that the shoulder detected in the first case can be better seen in the DTA curve, as a peak at 210°C, showing that DTA is a more sensitive technique than DSC to detect the beginning of the hematite formation. The first DTA peak or the shoulder DSC can be assigned to the production of hematite on the surface of the particles since it is expected that the reaction begins in the border of the particle [13]. To estimate roughly the average size of the N410 particles we applied the Collective Magnetic Excitation (CME) model [14], assuming that all the magnetic hyperfine field diminution, in comparison with α -Fe₂O₃ bulk, is originated in the reduced crystalline size. The average size obtained following this methodology was about 15 nm.

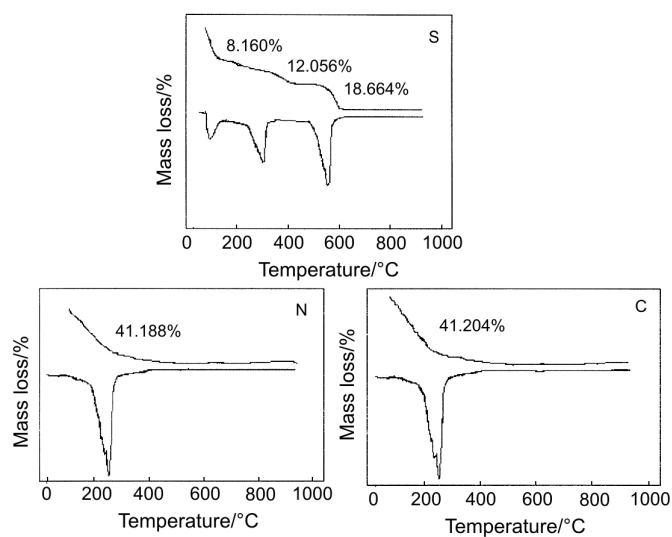


Fig. 3a TG curves of iron oxyhydroxide prepared with iron nitrate (N sample), iron sulfate (S sample) and iron chloride (C sample)

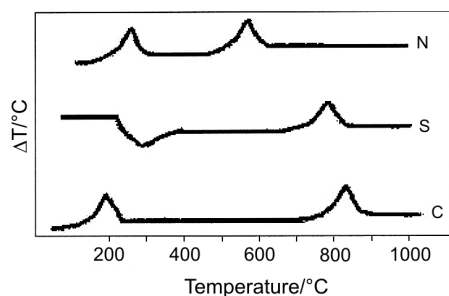


Fig. 3b DTA curves of iron oxyhydroxide prepared with iron nitrate (N sample), iron sulfate (S sample) and iron chloride (C sample)

Table 1a Mössbauer parameter of the sample prepared from iron nitrate (N sample) taken from the spectrum recorded at 298 K

Species	Parameters	N150	N250	N310	N410
Fe(III)hydrite (sp)	$\Delta/\text{mm s}^{-1}$	0.69 ± 0.01	0.72 ± 0.01	0.75 ± 0.01	–
$\approx\text{Fe}_5(\text{OH})_8\cdot 4\text{H}_2\text{O}$	$\delta/\text{mm s}^{-1}$	0.30 ± 0.01	0.30 ± 0.01	0.28 ± 0.01	–
	H/T	–	–	502 ± 1	504 ± 1
$\alpha\text{-Fe}_2\text{O}_3$	$\delta/\text{mm s}^{-1}$	–	–	0.34 ± 0.02	0.31 ± 0.01
	$2\varepsilon/\text{mm s}^{-1}$	–	–	-0.26 ± 0.04	-0.22 ± 0.04

H – hyperfine magnetic field (Teslas); δ – isomer shift (all the isomer shifts are referred to $\alpha\text{-Fe}$ at 298 K); 2ε – electrical quadrupole interaction; Δ – quadrupole splitting, (sp) – superparamagnetic

Table 1b Mössbauer parameter of the sample prepared from iron nitrate (N sample) taken from the spectrum recorded at 22 K

Species	Parameters	N150	N250	N310
Magnetic	H_{max}/T	453 ± 1	477 ± 1	484 ± 1
Fe(III)hydrite	$\langle H \rangle/\text{T}$	415 ± 1	459 ± 1	479 ± 1
$\approx\text{Fe}_5(\text{OH})_8\cdot 4\text{H}_2\text{O}$	$\delta/\text{mm s}^{-1}$	0.46 ± 0.01	0.46 ± 0.02	0.46 ± 0.01
	$2\varepsilon/\text{mm s}^{-1}$	-0.01 ± 0.01	-0.02 ± 0.01	-0.02 ± 0.02

H_{max} – maximum of the distribution of the hyperfine magnetic field (Teslas);

$\langle H \rangle$ – average of the distribution of the hyperfine magnetic field (Teslas);

δ – isomer shift (all the isomer shifts are referred to $\alpha\text{-Fe}$ at 298 K);

2ε – electrical quadrupole interaction

The sample prepared from iron sulfate showed a DSC curve with an endothermic peak at temperatures below 150°C and a shoulder at around 250°C. No significant change of surface area was noted in this range of temperature. From the DTA curve one can detect a peak which can be assigned to the loss of volatile in accordance with the TG curve. The X-ray diffractograms of the S150 and S310 samples showed two amorphous halos as shown in Fig. 2. The Mössbauer spectra of these samples showed a quadrupole doublet at room temperature and a very broad magnetic sextet at 22 K. Analyzing these results in a similar way to the N samples, we conclude that S150 and S310 are also Fe(III)hydrite (Tables 2a and 2b). However, the particle sizes and the crystallinities are lower than that the corresponding N samples. This conclusion is supported by the hyperfine magnetic fields in the S150 and S310 samples which are lower, and whose lines are wider, than in the N150 and N310 samples.

Heating the solid at 510°C, one can detect hematite by X-ray technique (Fig. 2). The Mössbauer spectrum of S510 at 298 K shows a central doublet and a magnetic sextet. Analyzing the Mössbauer parameters (Table 2a), the sextuplet can be assigned to hematite [10], while the central doublet can be attributed to very small hematite particles with a superparamagnetic relaxation. The last assignment was confirmed by the spectrum at 22 K (Table 2b). It displayed two magnetic signals, assignable to the ‘core’ and the ‘shell’ of hematite nanoparticles [15]. Assuming homogeneous spheri-

Table 2 Mössbauer parameter of the sample prepared from iron chloride (C sample) taken from the spectrum recorded at 298 K

Species	Parameters	C150	C410	C510
α -Fe ₂ O ₃ (sp)	$\Delta/\text{mm s}^{-1}$	–	0.67±0.01	–
	$\delta/\text{mm s}^{-1}$	–	0.34±0.01	–
	H/T	511±1	504±1	514±1
α -Fe ₂ O ₃	$\delta/\text{mm s}^{-1}$	0.37±0.01	0.37±0.01	0.37±0.01
	$2\epsilon/\text{mm s}^{-1}$	–0.22±0.01	–0.22±0.02	–0.22±0.01

H – hyperfine magnetic field in Teslas; δ – isomer shift (all the isomer shifts are referred to α -Fe at 298 K); 2ϵ – electrical quadrupole interaction; Δ – quadrupole splitting, (sp) – superparamagnetic

cal particles and using the ratio of the areas of the two sextuplets, it was possible to estimate an average nanoparticle diameter of 3.3 nm [15].

The sample prepared from iron chloride also showed a DSC curve with an endothermic peak at temperatures below 150°C (Fig. 1). The sample heated at this temperature showed a specific area of 192 m² g⁻¹ and the X-ray diffractogram showed two amorphous halos (Fig. 2). The Mössbauer spectrum of C410 at room temperature shows a central doublet and a magnetic sextet. The magnetic fraction represents 18% of the total area, and analyzing their Mössbauer parameters this signal can be assigned to hematite (Table 3). The central doublet would be a very small superparamagnetic hematite particles or Fe(III)hydrite. The Mössbauer spectrum of C510 at room temperature only shows a signal magnetically splitted with hyperfine parameters typical of hematite [10] (Table 3). Applying the CME model an average particle size of about 24 nm was obtained. From 150 to 410°C, there was a strong loss of mass and at this temperature the solid showed a smaller specific area showing that this process was followed by coalescence of particles and porous. In the range of 410 to 510°C no significant loss of mass and change in the specific area were noted.

The amounts of nitrogen, sulfur and chloride in the samples are shown in Fig. 1. It can be seen that very small amounts of nitrate remained in the solid heated at 150°C and there was no nitrate at 450°C. This can be assigned to the weakness of the Fe-NO₃⁻ bonds in solids. On the other hand, chloride and sulfate are strongly bounded and will not be easily removed from the solids, as shown the results of chemical analysis (Fig. 1). These results suggest that sulfur and chloride acts as impurities affecting the thermal decomposition of iron oxides. This can be explained by considering that they decrease the mobility of the species for reacting and crystallizing.

Conclusions

The use of different precursors affects the thermal curves of the thermal decomposition of iron oxyhydroxides. When iron nitrate is used, the production of hematite begins at around 250°C from Fe(III)hydrite; it would correspond to the oxide produced

in the external part of the particle and can be detected as a shoulder in the DSC curve and as a peak in DTA curve. When the precursors of the iron oxyhydroxides are sulfate or chloride the beginning of hematite formation occurs at higher temperatures. This can be assigned to strong Fe-sulfate and Fe-chloride bonds which decrease the mobility of the species for reacting and crystallizing. Besides, there is a pronounced effect of the iron precursor on the final particle diameters. Thus:

$$D_{\text{sulfate precursor}}(3.3 \text{ nm}) \ll D_{\text{nitrate precursor}}(15 \text{ nm}) < D_{\text{chloride precursor}}(24 \text{ nm})$$

Therefore, it was demonstrated the influence of the iron oxyhydroxide precursors on the textural properties of the final hematite, in accordance with previous works carried out with other precursors [16, 17]. This conclusion is very important in technologic applications of the hematite, for example, in some chemical reactions in which the particle size plays an essential role when this solid is used as a catalyst.

* * *

The authors thank the financial support from PADCT/FINEP/CNPq. A.C.O. acknowledges CNPq for her graduate scholarship.

References

- 1 A. Navrotsky, *J. Therm. Anal. Cal.*, 57 (1999) 653.
- 2 J. Orewczk, *J. Therm. Anal. Cal.*, 60 (2000) 265.
- 3 K. Przepiera and A. Przepiera, *J. Therm. Anal. Cal.*, 65 (2001) 497.
- 4 A. Nielsen and H. Bohlbro, *An Investigation on Promoted Iron Catalysts for the Synthesis of Ammonia*, Gjellerup Forlag, Copenhagen 1968, p. 221.
- 5 M. V. Twigg, L. Lloyd and D. E. Ridler, *Catalyst Handbook*, Manson Publishing Ltd., London 1996, p. 339.
- 6 J. L. R. Costa, G. S. Marchetti and M. C. Rangel, *Catal. Today*, 77 (2002) 205.
- 7 M. E. Dry, *The Sasol Fisher-Tropsch Processes* in B. F. Leach (Ed.), *Applied Industrial Catalysis*, Academic Press, New York 1983, p.177.
- 8 J. Bassett, R. C. Denney, G. H. Jeffery and J. Mendhan, *Vogel's A. J.: A Textbook of Practical Inorganic Qualitative Chemistry*, Longman, 1978, p. 372, 446.
- 9 E. Murad, L. H. Bowen, G. J. Long and T. G. Quin, *Clay Minerals*, 23 (1988) 161.
- 10 R. E. Vandenberghe, *Mössbauer Spectroscopy and Applications in Geology*, International Training Centre for Post-Graduate Soil Scientists, Belgium 1991.
- 11 M. C. Rangel and F. Galembeck, *J. Catal.*, 145 (1994) 364.
- 12 Y. Ichiyangi and Y. Kimishima, *J. Therm. Anal. Cal.*, 69 (2002) 919.
- 13 R. Furuichi, M. Hachia and T. Ishii, *Thermochim. Acta*, 4 (1988) 13.
- 14 S. Mørup and H. Topsøe, *Appl. Phys.*, 11 (1976) 63.
- 15 M. Vasquez-Mansilla, R. D. Zysler, C. Arciprete, M. I. Dimitrijewits, C. Saragovi and J. M. Greneche, *J. Magn. Magn. Mater.*, 204 (1999) 29.
- 16 I. Mitov, D. Paneca and B. Kunev, *Thermochim. Acta*, 386 (2002) 179.
- 17 N. Koga, S. Takemoto, T. Nakamura and H. Tanaka, *Thermochim. Acta*, 282 (1996) 81.